



A closed form for the Stress Intensity Factor of a small embedded square-like flaw

Paolo Livieri, Fausto Segala

University of Ferrara, Department of Engineering, Italy

paolo.livieri@unife.it, fausto.segala@unife.it



ABSTRACT. In the present work, the stress intensity factor (SIF) of a small embedded square-like flaw is calculated by means of a procedure based on the Oore-Burns integral. An explicit equation is given to evaluate the SIF along the two axes of symmetry that correspond to the points where the SIF takes its maximum and minimum value on the contour crack. The SIF is calculated in accordance with FE numerical results.

KEYWORDS. Weight function; Stress intensity factor; Three-dimensional crack; weld

Citation: Livieri, P., Segala, F., A closed form for the Stress Intensity Factor of a small embedded square-like flaw, *Frattura ed Integrità Strutturale*, 54 (2020) 182-191.

Received: 20.08.2020

Accepted: 26.08.2020

Published: 01.10.2020

Copyright: © 2020 This is an open access article under the terms of the CC-BY 4.0, which permits unrestricted use, distribution, and reproduction in any medium, provided the original author and source are credited.

INTRODUCTION

The analytical evaluation of the stress intensity factor (SIF) of three-dimensional cracks is more complicated than cases where the crack is sketched as a straight line in a two-dimensional boundary. Few examples of convex three-dimensional cracks can be found in textbooks [1–3]. In order to give a general formulation for the SIF, Bueckner [4] and Rice [5] performed the weight function technique. In this way, the calculation is reduced to an integral exactly over the region covered by the crack and this becomes particularly useful in the case of three-dimensional cracks. The exact weight function is known only in few cases. Galin evaluated the exact weight function for the circle but the equation is not simple to manage due to the presence of a singularity typical of the weight function itself (see reference [3]). However, the authors, by means of the Oore-Burns (OB) weight function, give a simplified formulation of the weight function of the analytical circle where the singularity disappears by means of an appropriate change of variable [6]. This was performed because the OB integral is exact on circles. In others cases, the OB integral is a first level of approximation for the SIF in the case of circle-like cracks [7].

Usually, for irregular contours, a crack-like elliptical crack can be adopted [8–9]. For example, in flaw characterisation adopted in the fitness-for-service procedure, the flaw is modelled by a simpler geometry such as a trough crack with a straight crack front or with an elliptical or semi-elliptical shape. In this cases, the OB integral should be adopted because the characterisation of a semi-axial ellipse (1, b), when eccentricity e tends to zero, the main contribution of the OB integral



differs from Irwin's analytical solution [11] for a small amount equal to $\frac{e^2}{20\sqrt{\pi}}$ [12], where e is the eccentricity of the ellipse.

The OB integral could also be useful in the fatigue life assessment of materials with small internal defects. In order to obtain an acceptable approximation of the maximum SIF $K_{I,max}$, Murakami took into account the square root of the crack area ($K_{I,max} = Y \sigma \sqrt{\pi \sqrt{area}}$ where Y is a coefficient that was evaluated as best fitting for numerical and analytical results; see also [13]) of a general crack shape. The internal defect often has rounded corners and an analytical equation for a square-like flaw could be useful for design purposes.

In this paper, we use the Oore-Burns integral to obtain a closed form solution for a square-like flaw that is intermediate from a circular flaw and a square crack. The results are then compared with the FE results obtained with a fine mesh.

WEIGHT FUNCTION FOR A THREE-DIMENSIONAL CRACK: ANALYTICAL BACKGROUND

Fig. 1 shows a two-dimensional crack inside a three-dimensional body subjected to a nominal tensile loading $\sigma_n(Q)$ that is evaluated without the presence of the crack. Q is the inner point of the crack. The crack can be considered as an open bounded simply connected subset Ω of the plane. We define:

$$f(Q) = \int_{\partial\Omega} \frac{ds}{|Q - P(s)|^2} \quad (1)$$

where $Q = Q(x, y) \in \Omega$, s is the arch-length parameter and point $P(s)$ runs over the boundary $\partial\Omega$. In their pioneering work in 1980, Oore-Burns [10] proposed the following expression for the mode I stress intensity factor (SIF) for a two-dimensional crack of boundary $\partial\Omega$:

$$K_I(Q') = \frac{\sqrt{2}}{\pi} \int_{\Omega} \frac{\sigma_n(Q)}{\sqrt{f(Q)} |Q - Q'|^2} d\Omega, \quad Q' \in \partial\Omega \quad (2)$$

Under reasonable hypothesis on the function $\sigma_n(Q)$, the integral (2) is convergent and the proof is based on the asymptotic behaviour of $f(Q)$ [14].

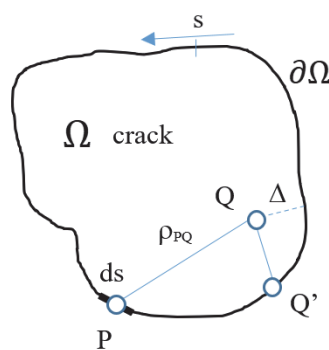


Figure 1: Inner crack.

STRESS INTENSITY FACTOR FOR A SQUARE LIKE-FLAW

In the case of a square-like flaw, as indicated in Fig. 2, the Oore-Burns integral can be analytically expressed in simplified form at the two points A and B. The Oore-Burns integral will be approximated by means of Riemann sums plus a

suitable asymptotic (in terms of mesh size) correction. The equation of a unitary square-like flaw in a Cartesian coordinate system x,y is given in the form:

$$x^4 + y^4 = 1 \tag{3}$$

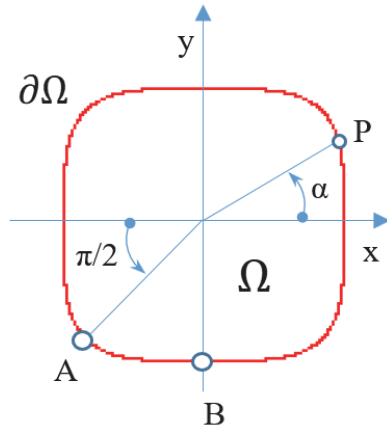


Figure 2: Square-like flaw

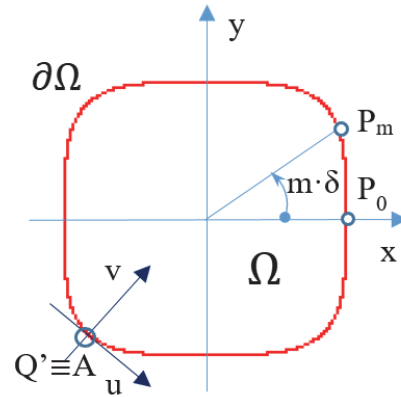


Figure 3: Auxiliary Cartesian plane u,v at point A

The choice to consider a unitary square-like flaw, as in Fig. 2, is not restrictive because the final values for the SIF can be recovered by multiplying by the square root of the geometrical scale factors.

Let us consider Q' as the point where the SIF is calculated. As a first calculation, we consider Q' as overlapping point A. In order to evaluate the O-B integral, we take into account a new convenient Cartesian orthogonal reference system u,v with its origin in Q' with a u axis tangent to $\partial\Omega$ (see Fig. 3).

The relation between the two reference planes can be summarised as follows:

$$x = \frac{1}{\sqrt{2}}(u + v - 2^{1/4}) \tag{4}$$

$$y = \frac{1}{\sqrt{2}}(-u + v - 2^{1/4}) \tag{5}$$

$$u = \frac{x - y}{\sqrt{2}} \tag{6}$$

$$v = \frac{x + y}{\sqrt{2}} + 2^{1/4} \tag{7}$$

A mesh of size δ on $\partial\Omega$ can be considered, where δ divides the length of $\partial\Omega$. P_m in Fig. 3 is a point of coordinate $m\delta$ with respect to the initial point P_0 . On the x,y plane, the coordinates of P_m are equal to $(x_m, y_m) = R(m\delta) (\cos(m\delta), \sin(m\delta))$ with m from 0 to M and $2M\delta = 2\pi$. From Eq. (3) we have:

$$R(\alpha) = \cos(\alpha)^4 + \sin(\alpha)^4 \tag{8}$$

If we know the polar equation of the crack border $R(\alpha)$, it is convenient to discretise the angle α instead of the arc length s . The angle α is equal to $m\delta$.

Now we consider:



$$\gamma(\alpha) = \sqrt{R^2(\alpha) + R^{12}(\alpha)} \tag{9}$$

The coordinates of generic point $P_m = (x_m, y_m)$ on the u, v plane become:

$$\begin{cases} u_m = \frac{1}{\sqrt{2}} R(m\delta)(\cos m\delta - \sin m\delta) \\ v_m = \frac{1}{\sqrt{2}} R(m\delta)(\cos m\delta + \sin m\delta) + 2^{1/4} \end{cases} \tag{10}$$

we denote by $Q_{jk} = k\delta(\cos(j\delta), \sin(j\delta))$ the generic point on the plane (u, v) of the semi-circular mesh (see Fig. 4). In order to establish whether point Q_{jk} of the coordinates (u, v) is inside the crack, the following inequality must be verified:

$$(u + v - 2^{1/4})^4 + (-u + v - 2^{1/4})^4 < 4 \tag{11}$$

In this paper, Eq. (11) is very simple to use with respect to the general equations proposed in references [15 and 16] for a star domain crack. From Eqns. (1) and (2), the SIF K_{IA} at point A results:

$$K_{IA} = \left(\frac{\sqrt{2}\sigma}{\pi} \sum \frac{A_{jk}}{k} + D \right) \sqrt{\delta} + O(\delta) \tag{12}$$

where

$$A_{jk} = \left(\sum |Q_{jk} - P_m|^{-2} \gamma\left(\frac{\pi}{4} + m\delta\right) \right)^{\frac{1}{2}} \tag{13}$$

The sum (12) is made for $1 < k < N$ and $0 < j < M/2$. The value of N is calculated in order to obtain a crack inside the mesh as appears in Fig. 4. The asymptotic correction term, according to reference [16] is given by:

$$D = 0.889 + 0.038 \gamma\left(\frac{\pi}{4}\right)^{\frac{3}{2}} \cos\left(\frac{2\pi}{\gamma\left(\frac{\pi}{4}\right)}\Gamma\right) \tag{14}$$

where $\Gamma = \max \gamma(\alpha)$, $\alpha \in [0, 2\pi]$.

Now we can evaluate the SIF also for point B as in Fig. 5. Eqns. (10)–(14) are replaced with Eqns. (15)–(19) and the mesh for Riemann sums is shown in Fig. 6.

$$\begin{cases} u_m = x_m = R(m\delta) \cos m\delta \\ v_m = R(m\delta) \sin m\delta + 1 \end{cases} \tag{15}$$

$$u^4 + (v - 1)^4 < 1 \tag{16}$$

$$K_{IB} = \left(\frac{\sqrt{2}\sigma}{\pi} \sum \frac{A_{jk}}{k} + D \right) \sqrt{\delta} \tag{17}$$

Where

$$A_{jk} = \left(\sum |Q_{jk} - P_m|^{-2} \gamma \left(\frac{\pi}{2} + m\delta \right) \right)^{-\frac{1}{2}} \tag{18}$$

The sum (17) is made for $1 < k < N$ and $0 < j < M/2$.

$$D = 0.889 + 0.038 \gamma \left(\frac{\pi}{2} \right)^{\frac{3}{2}} \cos \left(\frac{2\pi}{\gamma \left(\frac{\pi}{2} \right)} \Gamma \right) \tag{19}$$

where $\Gamma = \max \gamma(\alpha)$, $\alpha \in [0, 2\pi]$.

In Eqns. (14) and (19), the value of Γ can be numerically evaluated from Fig. 7. Γ is close to 1.265.

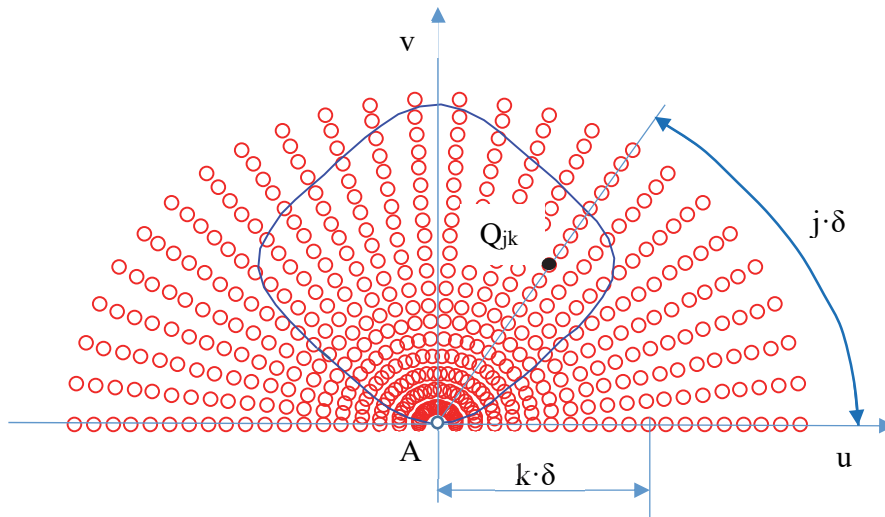


Figure 4: Mesh for Riemann sums at point A

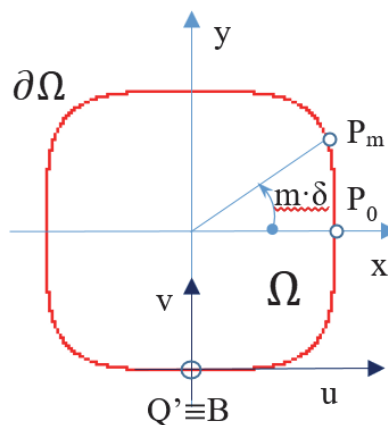


Figure 5: Auxiliary Cartesian plane u,v at point B

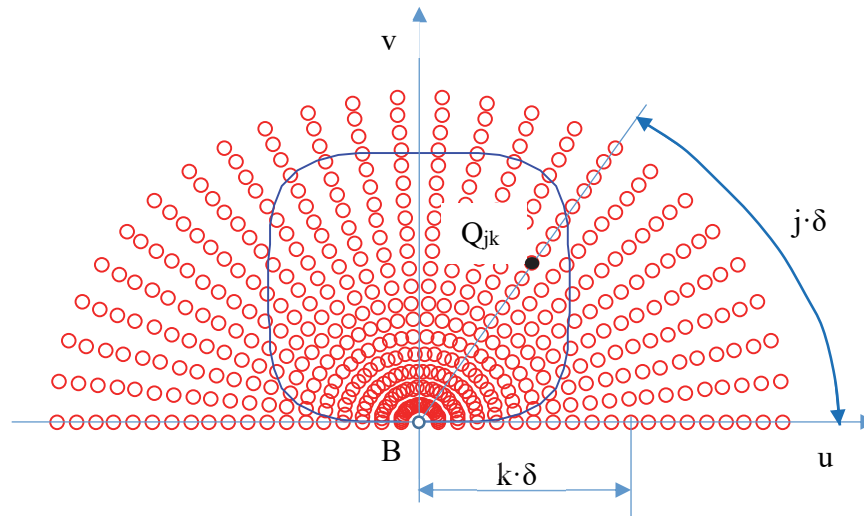


Figure 6: Mesh for Riemann sums at point A

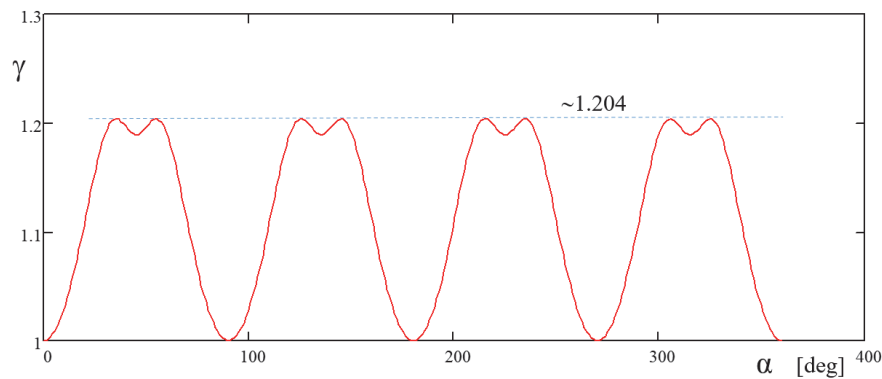


Figure 7: Trend of γ along the crack border

NUMERICAL VALIDATION

Eqns. (12) and (17) allow us to numerically evaluate the SIF at the two characteristic points A and B of the square-like crack without any specific computer strategies [17]. In this case, any generic mathematical code can be used to calculate the SIF. Tabs. 1 and 2 report the value obtained with Eq. (12) and (17). The stability of the equation is clear as well as the fundamental rule of asymptotic term C.

Mastrojannis et al. [18] numerically solved the case of square crack with a small rounded apex. They found that the maximum SIF was assumed to be at the middle point of the edge and the maximum shape factor $Y_{\max} = K_{I,\max} / (\sigma \sqrt{\pi a})$ was equal to 0.76. Furthermore, for a sharp square crack by means of numerical methods, Helsing et al. [19] calculated a value for Y_{\max} equal to 0.75, Weaver [20] gave 0.74, whereas Isida et al. [21] gave 0.76.

The results relating to a square-like crack are compared with those obtained by means of the FE code. The percentage of errors are around a few per cent for point B, while they increase up to 10% for point A.

Figs. 8 and 9 show the model and the mesh used in the numerical FE analysis. The mesh used in this work is accurate as proposed in previous works [22–25]. The dimensions of smaller elements at the tip of the crack were in the order of 10^{-5} mm. Fig. 10 highlights that the slope of stress σ_z in a double logarithm scale is close to the theoretical value of 0.5 for point B [26]. The y' axis has the origin at point B.

Regarding the engineering applications for this topic, the fatigue behaviour of welded joints with internal defects such as pores could be appropriate. For example, the morphology and size distribution of gas pores within the entire weld joints, were examined in references [27–28]. By observing the typical spatial shape of the defects, sometime, the square-like flaw

appears more appropriate than others shapes when a two-dimensional simplified representation of the defects is requested [13]. The pores show a rounded shape sometime away any ellipse typically used for simplified fatigue assessment [8].

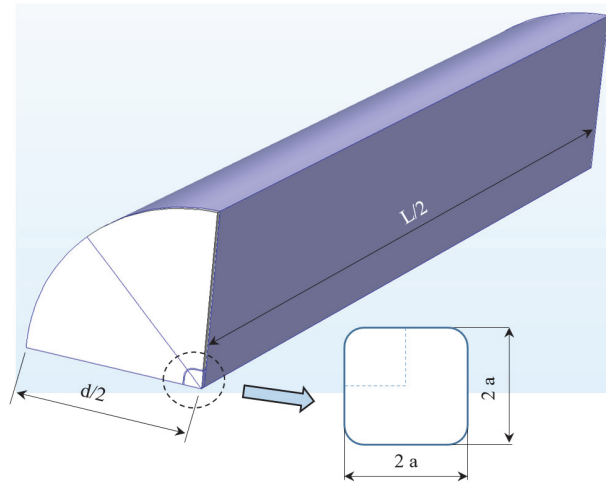


Figure 8: Three-dimensional model for a square-like crack ($a=1$ mm, $L/a=100$, $d/a=20$).

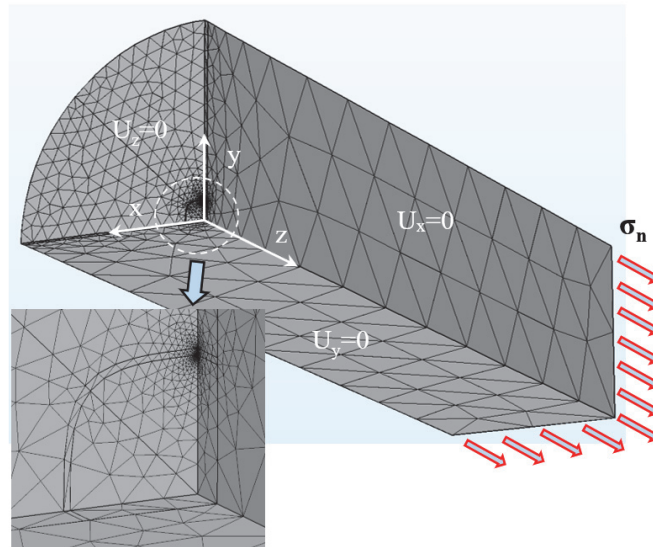


Figure 9: Mesh and boundary conditions for a square-like crack of Fig. 8.

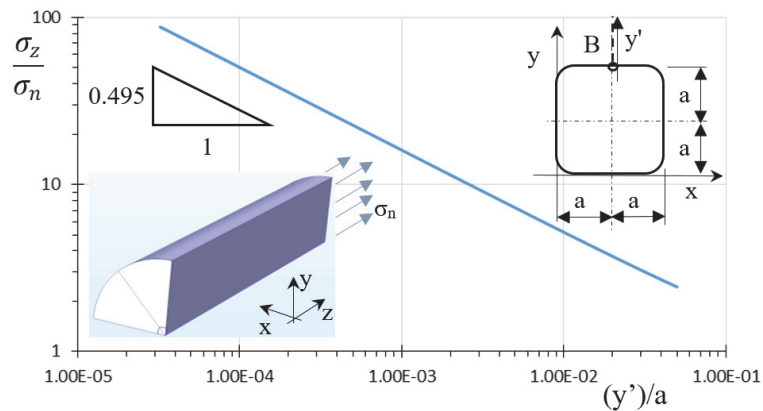
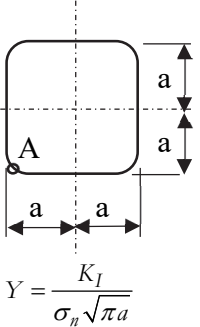
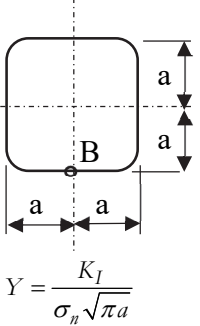


Figure 10: Stress σ_z along the y -direction for the square-like crack of Fig. 4 for B on the symmetry axis

M	δ	Y Riemann Sum	Y Asymptotic term	Y Eq. (12)	Y FE	e%
10	0.628	0.246	0.418	0.664	0.554	-19.8
20	0.314	0.335	0.295	0.630	0.554	-13.7
50	0.126	0.428	0.187	0.615	0.554	-11.0
100	0.063	0.483	0.133	0.616	0.554	-11.1
200	0.031	0.520	0.094	0.614	0.554	-10.8

Table 1: Shape factor at point A for a nominal tensile loading σ_n



M	δ	Y Riemann Sum	Y Asymptotic term	Y Eq. (17)	Y FE	e%
10	0.628	0.300	0.398	0.698	0.717	2.6
20	0.314	0.416	0.282	0.698	0.717	2.6
50	0.126	0.537	0.179	0.716	0.717	0.1
100	0.063	0.579	0.127	0.706	0.717	1.5
200	0.031	0.617	0.090	0.707	0.717	1.3

Table 2: Shape factor at point B for a nominal tensile loading σ_n

CONCLUSIONS

The Oore-Burns weight function gives us a closed formula for the estimation of the stress intensity factor of a square-like flaw with a rounded corner. The errors, with respect to the FE results, are around a few per cent in the middle of the side, while they increase up to 10% at the corner. This suggests the need for a corrective procedure in order to significantly improve the Oore-Burns integral. After careful investigations, it is now clear, without any doubt, that the accuracy of the integral is not satisfactory at the high curvature points of the crack.

NOMENCLATURE

- a crack size
- δ size of mesh over crack
- Y shape factor
- Ω crack shape
- $\partial\Omega$ crack border
- Q point of Ω
- Q' point of crack border
- Δ distance between Q and $\partial\Omega$
- K_I mode I stress intensity factor
- x, y actual Cartesian coordinate system



u, v	auxiliary coordinate system
ρ	polar radius
R	polar radius for the square-like flaw
s	arc length
σ_n	nominal tensile stress in x, y Cartesian coordinate system

REFERENCES

- [1] Murakami, Y. (Chief ed) (2001), *Stress Intensity Factors Handbook Vol. 4, 5*, Pergamon. Press, Oxford, U.K.
- [2] Fett, T., Munz, D., (1997). *Stress intensity factors and weight functions*, Computational Mechanics Publications.
- [3] Tada, H., Paris, C.P., Irwin, G.R., (2000). *The stress analysis of cracks handbook*. Third edition, ASME press.
- [4] Bueckner, H.F., (1970). A novel principle for the computation of stress intensity factors, *ZAMM* 50, pp. 529–546.
- [5] Rice, J.R., (1989). Weight function theory for three-dimensional elastic crack analysis. ASTM STP1020, Wei R.P. and Gangloff R.P., Eds. Philadelphia, American Society for Testing and Materials, pp. 29–57.
- [6] Livieri, P., Segala, F., (2010). An analysis of three-dimensional planar embedded cracks subjected to uniform tensile stress. *Engineering Fracture Mechanics*, 77, pp. 1656–1664.
- [7] Livieri, P., Segala, F., (2010). First order Oore–Burns integral for nearly circular cracks under uniform tensile loading. *International Journal of Solids and Structures*, 47(9), pp. 1167–1176.
- [8] Zerbs, U. T., Schödel, M., Webster, S., Ainsworth, R. (2007). *Fitness-for-Service Fracture Assessment of Structures Containing Cracks: A Workbook based on the European SINTAP/FITNET procedure*, Elsevier, 1st ed. Oxford, Amsterdam, The Netherlands .
- [9] Hobbacher, A., (1995). Recommendation on fatigue of welded components. IIW Document XIII-1539-95/XV-845-95.
- [10] Oore, M., Burns, D.J., (1980). Estimation of stress intensity factors for embedded irregular cracks subjected to arbitrary normal stress fields. *Journal of Pressure Vessel Technology ASME*, 102, pp. 202–211.
- [11] Irwin, G.R., (1962). Crack-extension force for a part-through crack in a plate. *ASME, Journal of Applied Mechanics*, 29(4), pp. 651–654.
- [12] Livieri, P., Segala F. (2015). New weight functions and second order approximation of the Oore-Burns integral for elliptical cracks subject to arbitrary normal stress field, *Eng. Fract. Mech.* 138, pp. 100–117.
- [13] Murakami, Y., (2002). *Metal Fatigue: Effects of small defects and non-metallic inclusions*, Elsevier.
- [14] Ascenzi, O., Pareschi, L., Segala, F. (2002). A precise computation of stress intensity factor on the front of a convex planar crack. *International Journal for numerical methods in Engineering* 54, pp. 241–261.
- [15] Livieri, P., Segala, F., (2014). Sharp evaluation of the Oore-Burns integral for cracks subjected to arbitrary normal stress field, *Fatigue & Fracture of Engineering Materials & Structures* 37, pp. 95–106.
- [16] Livieri, P., Segala, F., (2018). An approximation in closed form for the integral of Oore–Burns for cracks similar to a star domain. *Fatigue Fract Eng Mater Struct*, 41, pp. 3–19.
- [17] Desjardins, J.L., Burns, D.J., Thompson, J.C., (1991). A weight function technique for estimating stress intensity factors for cracks in high pressure. *Journal of Pressure Vessel Technology, ASME*, 113, pp. 10–21.
- [18] Mastrojannis, E.N., Keer, L.M., Mura, T., (1979). Stress intensity factor for a plane crack under normal pressure. *International Journal of Fracture*, 15 (3), pp. 247–258.
- [19] Helsing J, Jonsson A, Peters G. (2001). Evaluation of the mode I stress intensity factor for a square crack in 3D, *Engineering Fracture Mechanics* 68, 605–612.
- [20] Weaver, J., (1997). Three-dimensional crack analysis. *International Journal Structures*, 13, pp. 321–330.
- [21] Isida, M., Yoshida, T., Noguchi, H. (1991). A rectangular crack in an infinite solid, a semi-infinite solid and a finite-thickness plate subjected to tension. *International journal of Fracture* 52, pp. 79–90.
- [22] Livieri, P., Tovo, R., (2009). The use of the J_v parameter in welded joints: stress analysis and fatigue assessment. *International Journal of Fatigue*, 31(1), pp. 153–163.
- [23] Livieri, P., Tovo, R., (2017). Analysis of the thickness effect in thin steel welded structures under uniaxial fatigue loading. *International Journal of Fatigue*, 101(2), pp. 363–370.
- [24] Livieri, P., Segala, S. (2016). Stress intensity factors for embedded elliptical cracks in cylindrical and spherical vessels *Theoretical and Applied Fracture Mechanics* 86(1), pp. 260–266.



- [25] Livieri, P., Berto, F., Lazzarin, P., (2007). Local strain energy approach applied to fatigue analysis of welded rectangular hollow section joints. *International Journal of Materials & Product Technology*, 30(1/2/3), pp. 124–140.
- [26] Aliabadi, M.H., Rooke, D.P., (1991). *Numerical Fracture Mechanics*, Southampton, Kluwer Academic Publishers.
- [27] Wu, S.C., Yu, C., Yu, P.S., Buffière, J.Y., Helfen, L., Fu., Y.N., (2016). Corner fatigue cracking behavior of hybrid laser AA7020 welds by synchrotron X-ray computed microtomography. *Materials Science&EngineeringA* 651, pp. 604–614.
- [28] Gou, G., Zhang, M., Chen, H., Chen, J., Li, P., Yang, Y.P., (2015). Effect of humidity on porosity, microstructure, and fatigue strength of A7N01S-T5 aluminum alloy welded joints in high-speed trains. *Materials and Design* 85, pp. 309–317.